p-ISSN 2089 – 0133 e-ISSN 2477-6416
URL : https://jurnal.uns.ac.id/ijap/article/view/67191
Indonesian Journal of Applied Physics (IJAP) Vol. 13 No. 2 page 201
DOI : https://doi.org/10.13057/ijap.v13i2.67191

# THE SPATIAL ARRANGEMENT OF THE ELECTRIC FIELD IN THE NEEDLE-PLATE ELECTROSPINNING

**Ahmad Kusumaatmaja*[1], Muhamad Nasrudin Manaf[1], Shiddiq Nur Hidayat[1], Kuwat Triyana[1], Farah Fahma[2], Grandprix T. M. Kadja[3], and Muchammad Yunus[4]**

[1]Department of Physics, Universitas Gadjah Mada, Bulaksumur 55281, Yogyakarta, Indonesia.
[2] Department of Agroindustrial Technology, Faculty of Agricultural Engineering and Technology, Bogor Agriculture University, Bogor, Indonesia
[3]Division of Inorganic and Physical Chemistry, Institut Teknologi Bandung, Bandung, Indonesia
[4]Faculty of Veterinary Medicine, Airlangga University, Surabaya, Indonesia
*ahmad_k@ugm.ac.id

Received 11-11-2022, Revised 19-09-2023, Accepted 08-10-2023
Available Online 08-10-2023, Published Regularly October 2023

## ABSTRACT

The electric field distribution of the Neddle-Plate (NP) electrospinning setup has been reported due to the simple classical electrodynamics solutions. The charge is assumed to distribute uniformly in the collector (plate) and needle (nozzle). The electric field is only influenced in the early stage of the electrospinning process. The electric field and the jet fluid's viscosity have caused the straight jet's bending. The high density of the fluid can preserve the direct jet length much longer. The electric field gives the initial angular momentum of the jet due to the whipping motion of the jet. The electric does not influence the whipping motion for the area away from the nozzle. Then, the whipping motion solely due to the influence of the charge repulsion of the jet fluid and the evaporation of the solvent.

Keywords: Electrospinning; nanofiber; electric field distribution

**Cited this as:** Kusumaatmaja, A., Manaf, M. N., Hidayat, S. N., Triyana, K., Fahma, F., Kadja, G. T. M., & Yunus, M. 2023. The Spatial Arrangement of The Electric Field in the Needle-Plate Electrospinning. *IJAP: Indonesian Journal of Applied Physics*, *13*(2), 201-206. doi: https://doi.org/10.13057/ijap.v13i2.67191

## INTRODUCTION

Electrospinning is a method to produce nanofibers by accelerating the jet of the electrically charged fluid of polymers at high voltage. The configuration of this system consists of the nozzle in which the fluid of the polymer is ejected and the collector[1]. The shape of the nozzle can be a needle, hole, or plate with a bulge in which the polymer is ejected, and almost the collector has a shape like a plate. Then, the electrospinning setup can be nozzle as needle-plate (NP), hole-plate (HP), and plate-plate (PP), respectively[1-2].

The nanofibers produced by electrospinning resulted in a smaller diameter than the fibers created by conventional methods[1-3]. The electrospinning method produced nanofibers in the range of micrometers until nanometer scale[3-5]. These small fibers are potentially using for many applications, such as membrane of filtration and composite materials[6-10]. Beside the size of the fibers, the electrospinning produces high surface area of threads. It has attractive as catalyst support and drug delivery[6, 10-12]. Mostly these nanofibers have used in many applications such as life science, medicine, and industry[6, 13-15].

Although many applications can be developed from the nanofibers produced by electrospinning, but the controlling fiber diameter remains obstacles. Many variables of the physical quantities have influenced the producing nanofibers in the electrospinning process. These physical quantities are from the set up of the electrospinning itself and the fluid of polymer. The physical quantities from the set up of the electrospinning are the electric field and distance between the nozzle to the collector[1-2, 16-18]. The physical quantities of the solution of polymer that influence the electrospinning are the viscosity, charge density, and evaporation rate [12, 16, 19-20].

The electric field was the crucial factor for controlling the diameter of the fiber in the electrospinning process. The different set up of the electrospinning produces different strength and uniformity. Based on the previous result that the PP system produces uniform electric field[1], while the other two systems in which HP and NP system produce a slightly non-uniform electric field and very nonuniform electric field respectively[1-2].

Previously, it was reported that the electric field's effect on the nanofibers' size was produced by the electrospinning method. Poly(ethylene oxide) (PEO) is a common polymer for electrospinning because it can spin at moderate voltages in direct current (DC) mode. Experiments with PEO aqueous solutions show that the uniformity of the electric field will affect the spinning results. Specifically, more uniform electric fields produce fibers due to the higher bending speed. Increasing the voltage on the electrospinning needle causes the change in the average electric field to be greater, resulting in a smaller fiber size[1].

Furthermore, Zheng et al. reported a comparative study between the HP and NP setup of the electrospinning[2]. Their results showed that an increased electric field at the spinneret produced a straighter jet and a smaller envelope cone for the needle-plate (NP) setup. In contrast, if the electric field intensity is uniform and higher and more uniform electric field intensity in the bending region of the hollow-needle (HP) arrangement, it produces tiny fiber diameters due to a higher flogging frequency, decreasing the velocity of the bending jet and increasing the jet path for stretching[2].

Although the NP showed the nonuniform electric filed, the NP set up remains interesting due to the lower operating voltage than the other set up of the electrospinning and simplicity to arrange this setup. However, the electric field distribution in the NP set up has not been fully discussed. In this paper, we report the analysis of electric field distribution in the NP set up that would influence the resulted fibers for certain applications.

## METHODS

The experimental set up of the NP electrospinning showed in Figure 1a. It consists of the needle with syringe pump in which the fluid of polymer is ejected. High voltage (HV) is used to generate the electric between the needle and the plate in which represented as anode and cathode or otherwise. Figure 1b shows the scheme of the NP set up in which $L, z_1, dq$ represents the length of the needle, controllable needle-to-collector distance and charge element, respectively. We consider that the diameter of the needle is much smaller than the area of the plate; therefore, the collector can be assumed as an infinite plate. The charge density in the needle and the collector are expected they distribute uniformly.

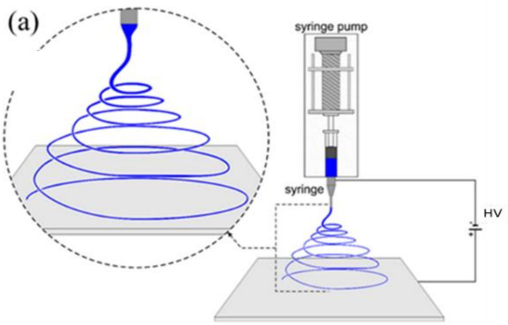


(a)

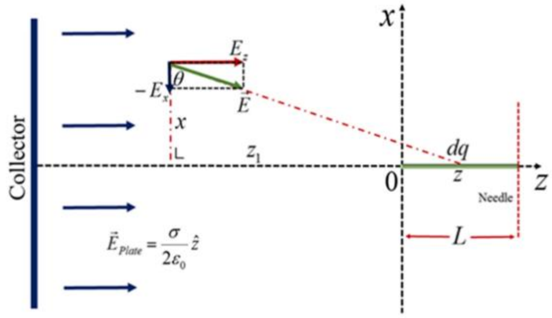


(b)

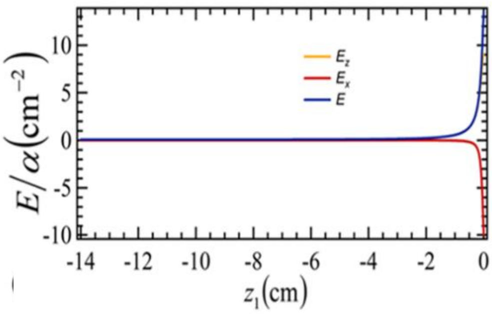


(c)

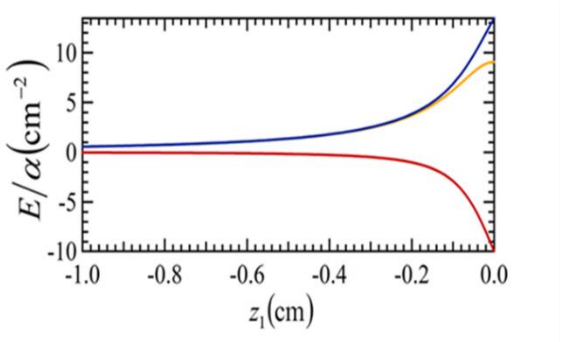


(d)

**Figure 1.** (a) The set up of the needle-plate (NP) electrospinning, (b) The scheme of the NP electrospinning, (c) The component and the modulus of the electric field between the needle and the plate, (d) The component and the modulus of the electric field near the tip of syringe..

## RESULTS AND DISCUSSION

Based on our model, we can construct the equation to represent the electric field of the NP electrospinning set up. The electric field consists of the vertical and radial components respectively. As shown in Figure 1, the vertical is represented by the z-components of the electrical field. Otherwise, the radial components are described by the x-components. The equations of the electric field components are as follow:

$$E_z = \frac{\sigma}{2\varepsilon_0} + \int_0^L \frac{(z - z_1)dz}{\left[x^2 + (z - z_1)^2\right]^{3/2}} \tag{1}$$

$$E_x = -k\lambda x \int_0^L \frac{dz}{\left[x^2 + (z - z_1)^2\right]} \tag{2}$$

in which $E_z$ and $E_x$ represent z-components and x-components of the electric field, respectively.While λ is the element charge of the needle and $k = 1/4\pi\varepsilon_0$ ( $\varepsilon_0$ is the permittivity of free space, $\varepsilon_0 \approx 8.85 \times 10^{-12}$ C2/N m2). The equation (1) and equation (2) representing the z and x components of the electric field respectively. The first component of the equation is the contribution from the collector, whereas the second component is from the needle. The equation (2) only get the contribution from the needle. The equation (1) and (2) can be solved as follows :

$$\frac{E_z}{\alpha} = \frac{1}{L}\left[\frac{-1}{\left((L-z_1)^2 + x^2\right)} + \frac{1}{\left(z_1^2 + x^2\right)}\right] + \frac{2\pi}{A} \tag{3}$$

$$\frac{E_x}{\alpha} = -\frac{1}{xL}\left[\frac{L-z_1}{\left((L-z_1^2)^2 + x^2\right)^{1/2}} + \frac{z_1}{\left(z_1^2 + x^2\right)^{1/2}}\right] \tag{4}$$

where $\alpha = kQ$ which represents the conductivity of materials. In our case we ignore the influence of the conductivity of the materials, which imply in equation (3) and equation (4), respectively. The plot of the equation (3) and equation (4) are shown in Figure 1c. The zoom of the electric field near the nozzle is shown in Figure 1d. From both figure we can confirm that the electric field has influenced only near the nozzle. The x-components dominantly affect the motion causing the bending of the jet fluid of the polymer. The jet of the fluid can pertain the longer straight shape depend on the viscosity of the liquid. The high viscosity of the polymer will produce longer straight path.

The Figure 2 shows the components of the electric field with the various distance of the needle. The electric field near the nozzle has a significant influence on the motion of the jet. The jet whipping of the motion is causing by the influence of the electric field, the repulsion charge in the fluid, and the evaporation. The components of the electric field contribute to the initial angular momentum for the motion of the jet. Then the influence of the electric field vanished, which the jet moves far away from the nozzle. The motion dominantly influences from the charge repulsion in the fluid and also from the evaporation. The radius of whipping becomes large, along with the moving away of the jet from the nozzle. The increasing radius of the whipping is caused by the reduction of the mass due to evaporation. The momentum conservation law then leads the increasing of the jet velocity. The increasing of the velocity due to reduction of the mass causing the jet take larger diameter of the motion than the before. The charge repulsion also gives the contribution in the process of the elongation of the jet. The interation between the same type of charge in jet fluid causing repulsion between the charge due the Coulombic Force. Both contributions from the evaporation and the repulsion of the charge give contributions to the final diameter of the fiber produced by electrospinning methods.

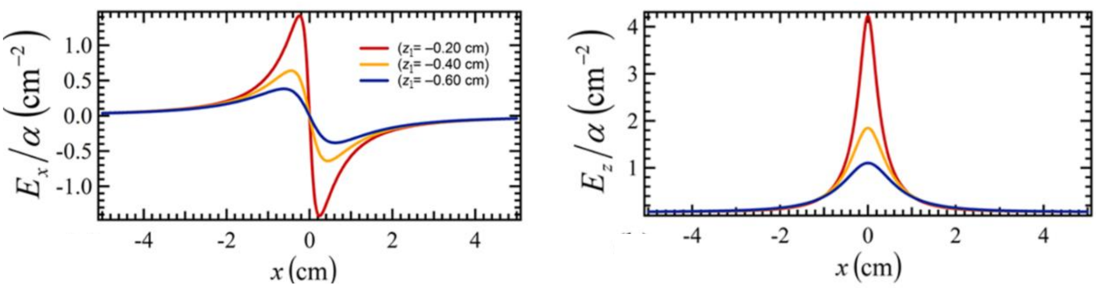


(a) (b)

**Figure 2**. (a) The x-component of the electric field and (b) the z-component of the electric field with the various distance from the needle.

## CONCLUSION

Based on our model, we can construct the equation to represent the electric field of the NP electrospinning set up. In this set up the electric field influence only in the near of the nozzle. The x-components of the electric field give control for the bending of the jet in the early stage of the electrospinning. The electric field also provides the initial angular momentum for the motion of the jet. In the area which far away from the nozzle, the electric field does not influence the motion of the jet. In this stage, the charge repulsion and the evaporation are dominantly influencing the motion of the jet.

NOMENCLATURE

| | | |
|---|---|---|
| $L$ | Length of the Needle | m |
| $Z_1$ | Controllable Distance Between the Needle to the Collector | m |
| $dq$ | Element of the Charge | C |
| $E_z$ | z-components of the electric field | N/m |
| $E_x$ | x-components of the electric field | N/m |

Greek letters

| | | |
|---|---|---|
| $\lambda$ | element charge of the needle | $Wm^{-2}K^{-1}$ |
| $\varepsilon_0$ | The Permittivity of Free Space | $C^2/N\ m^2$ |

## ACKNOWLEDGMENTS

This study was supported by the grants from the RKI (Riset Kolaborasi Indonesia). The authors are grateful for financial support from the Republic of Indonesia's Ministry of Research, Technology and Higher Education.

## REFERENCES

1 Xue, J., Wu, T., Dai, Y., & Xia, Y. 2019. Electrospinning and electrospun nanofibers: Methods, materials, and applications. *Chemical reviews, 119*(8), 5298-5415.

2 Zheng, Y., Xie, S., & Zeng, Y. 2013. Electric field distribution and jet motion in electrospinning process: from needle to hole. *Journal of Materials Science*, *48*(19), 6647-6655.

3 Stachewicz, U., Szewczyk, P. K., Kruk, A., Barber, A. H., & Czyrska-Filemonowicz, A. 2019. Pore shape and size dependence on cell growth into electrospun fiber scaffolds for tissue engineering: 2D and 3D analyses using SEM and FIB-SEM tomography. *Materials Science and Engineering: C, 95*, 397-408.

4 Riwu, Y. F., Loi, F. H. P., Kusumaatmaja, A., Roto, & Triyana, K. 2016. Effect of Chitosan concentration and heat treatment on electrospun PVA/Chitosan nanofibers. *AIP Conference Proceedings, 1755*(1), 150012.

5 Kusumaatmaja, A., Fauji, N., & Triyana, K. 2017. Polysulfone/Polyacrilonitrile Membrane for Oil/Water Separation. In *Materials Science Forum* (Vol. 886, pp. 145-149). Trans Tech Publications Ltd.

6 Hrib, J., Sirc, J., Hobzova, R., Hampejsova, Z., Bosakova, Z., Munzarova, M., & Michalek, J. 2015. Nanofibers for drug delivery–incorporation and release of model molecules, influence of molecular weight and polymer structure. *Beilstein journal of nanotechnology, 6*(1), 1939-1945.

7 Namekawa, K., Schreiber, M. T., Aoyagi, T., & Ebara, M. 2014. Fabrication of zeolite–polymer composite nanofibers for removal of uremic toxins from kidney failure patients. *Biomaterials Science, 2*(5), 674-679.

8 Zahari, A. M., Yusoff, A. R. M., Buang, N. A., Satishkumar, P., Jasni, M. J. F., & Yusop, Z. 2015. Fabrication and characterization of polyvinylidene fluoride composite nanofiber membrane for water flux property. *Jurnal Teknologi*, *74*(11).

9 Rianjanu, A., Roto, R., Julian, T., Hidayat, S. N., Kusumaatmaja, A., Suyono, E. A., & Triyana, K. 2018. Polyacrylonitrile nanofiber-based quartz crystal microbalance for sensitive detection of safrole. *Sensors*, *18*(4), 1150.

10 O'Connor, R. A., & McGuinness, G. B. 2016. Electrospun nanofibre bundles and yarns for tissue engineering applications: A review. *Proceedings of the Institution of Mechanical Engineers, Part H: Journal of Engineering in Medicine*, *230*(11), 987-998.

11 Ismaya, E. P., Diantoro, M., Kusumaatmaja, A., & Triyana, K. 2017. Preparation of PVA/TiO2 composites nanofibers by using electrospinning method for photocatalytic degradation. In *IOP Conference Series: Materials Science and Engineering*, *202*(1), 012011.

12 Rogina, A. 2014. Electrospinning process: Versatile preparation method for biodegradable and natural polymers and biocomposite systems applied in tissue engineering and drug delivery. *Applied Surface Science, 296*, 221-230.

13 Zheng, X., Shen, Z. P., Shi, L., Cheng, R., & Yuan, D. H. 2017. Photocatalytic membrane reactors (PMRs) in water treatment: configurations and influencing factors. *Catalysts*, *7*(8), 224.

14 Mertaniemi, H., Escobedo-Lucea, C., Sanz-Garcia, A., Gandía, C., Mäkitie, A., Partanen, J., & Yliperttula, M. 2016. Human stem cell decorated nanocellulose threads for biomedical applications. *Biomaterials*, *82*, 208-220.

15 Li, C., Fu, R., Yu, C., Li, Z., Guan, H., Hu, D., & Lu, L. 2013. Silver nanoparticle/chitosan oligosaccharide/poly (vinyl alcohol) nanofibers as wound dressings: a preclinical study. *International journal of nanomedicine*, *8*, 4131.

16 Yang, X., Wang, J., Guo, H., Liu, L., Xu, W., & Duan, G. 2020. Structural design toward functional materials by electrospinning: *A review. e-Polymers, 20*(1), 682-712. doi:10.1515/epoly-2020-0068

17 Stepanyan, R., Subbotin, A., Cuperus, L., Boonen, P., Dorschu, M., Oosterlinck, F., & Bulters, M. 2014. Fiber diameter control in electrospinning. *Applied Physics Letters*, *105*(17), 173105.

18 Jiang, J. G., Duan, H. W., He, T. H., & Li, B. 2015. Electric field simulation and experimentation of needle-plate type electrospinning machine. *Journal of Computational and Theoretical Nanoscience*, *12*(9), 2016-2022.

19 Wang, Y., & Wang, C. 2021. Extension rate and bending behavior of electrospinning jet: The role of solution conductivity. *Polymer, 222*, 123672.

20 Puspitasari, I., Diantoro, M., Kusumaatmaja, A., & Triyana, K. 2017. Effect of blend ratio on morphology and swelling properties of PVA/chitosan nanofibers. *Materials Science Forum*, *=901*, 79-84.